

# The properties of cuspy triaxial systems formed due to the radial-orbit instability

T. Piffl<sup>1</sup> and N. Ya. Sotnikova<sup>2</sup>

<sup>1</sup> Faculty of Physics, University of Leipzig, Linnestrasse 5, 04103 Leipzig, Germany  
e-mail: til@aip.de

<sup>2</sup> Sobolev Astronomical Institute, St. Petersburg State University, Universitetskij pr. 28, 198504 St. Petersburg, Stary Peterhof, Russia  
e-mail: nsot@astro.spbu.ru

Received ????, 2008; accepted ????, 2008

## ABSTRACT

*Context.* We have investigated the structure and kinematics of triaxial final models formed due to radial-orbit instability from a set of equilibrium anisotropic spherical systems of the Osipkov-Merritt type.

*Aims.* We show that the instability is a natural way to build nonspherical systems and thus can be considered as a new technique for constructing equilibrium  $N$ -body models.

*Methods.* The dynamical evolution of the models was followed numerically by means of the Dehnen's public code `gyrfacON`.

*Results.* We found that the shape of the density profiles for various initial spherical models didn't change despite of the systems were drastically rearranged into triaxial configurations and had got the new scale lengths. The cusp was found to be an invariant feature of such a rearranging. Starting from a certain unstable spherical  $\gamma$ -model we obtain a triaxial system with the same cusp. The end-products are anisotropic at large radii and have anisotropy profiles of the Osipkov-Merritt type. The size of the isotropic core once rescaled corresponds to the value of marginally stable  $\gamma$ -progenitors and is almost independent of the unstable starting point.

*Conclusions.* We conclude that the end-products reach a new steady state and have quite predictable properties. They can be used as equilibrium models to describe the elliptical galaxies and bulges. They also can be incorporated in  $N$ -body simulations deal with multicomponent systems.

**Key words.** stellar dynamics — instabilities — methods:  $N$ -body simulations — galaxies: structure — galaxies: kinematics and dynamics

## 1. Introduction

Triaxiality is very widespread among stellar systems. For example, there are a few perfectly spherical elliptical galaxies. The analysis of their morphology and kinematics have shown that ellipticals are at least moderately triaxial systems (Franx et al. 1991). Dark matter haloes formed in isolation (e.g., Aguilar & Merritt & 1990; Dubinski & Carlberg 1991; Katz 1991) or in subregions of larger cosmological simulations (e.g., Frenk et al. 1988; Warren et al. 1992) through dissipationless collapse of density peaks also demonstrate triaxial shapes. The same picture arises in cosmological simulations with halo assembling via merging (see, e.g., Jing & Suto 2002; Bailin & Steinmetz 2005; Shaw et al. 2006; Allgood et al. 2007; Bett et al. 2007).

There is one more common feature of real and cosmologically motivated systems. It is a lack of constant density cores. As a rule such systems have cuspy density profiles. The stellar surface brightness of early-type galaxies very often continues to rise towards small distances from the centre (Ferrarese et al. 1994; Lauer et al. 1995). But even a core-like surface brightness distribution can be transformed due to projection into a power-law cusp in its spatial density (Lauer et al. 1995). As is known for dark matter haloes those have universal cuspy density distributions — the so-called NFW profiles with  $\rho \propto r^{-\gamma}$  near the centre, where  $\gamma = 1$  (Navarro et al. 1996, 1997).

It is very important to have different reliable prescriptions for constructing equilibrium models of such systems and to know

their structural and dynamical properties. There are at least two problems which require such models. One of them deals with photometric and kinematic data fitting. The other includes many question connected with dynamical evolution of triaxial stellar systems in a controlled manner and related topics (e.g., the effects of triaxial halo shape on the disk stability and bar evolution, the survival of triaxiality during the disk formation and so on). The most practical models to solve the later tasks are  $N$ -body realizations of stellar systems. There are various and well developed techniques for constructing equilibrium models, mainly invented for spherical ones with known DF (for the DF construction of models with given density and velocity anisotropy profiles see Osipkov 1979; Merritt 1985a,b; Cuddeford 1991; Baes & Dejonghe 2002; Baes & Van Hese 2007), or for the superposition of spherical (or spheroid) and disk components (e.g., Hernquist 1993; Boily et al. 2001; Kuijken & Dubinski 1995; Widrow & Dubinski 1995; McMillan & Dehnen 2007; Rodionov et al. 2008).

To build triaxial models with given structural and kinematic parameters is a far more complicated problem. Jeans theorem and a knowledge of the DF is useful only in a few special analytical cases. The most popular numerical technique for triaxial system modelling is Schwarzschild's method (Schwarzschild 1979). Tested initially on core-like systems (Schwarzschild 1979; Statler 1987) it was further applied to obtain self-consistent galaxy models with cusps (Merritt & Fridman 1996; Merritt 1997) and recently has been generalized to construct models of triaxial elliptical galaxies embedded in triaxial dark

matter haloes (Capuzzo-Dolcetta et al. 2007). These models based on a library of orbits in a given potential are well suited to investigate the variety of orbit types presented in a model but have almost never been used to produce initial conditions for  $N$ -body simulations so far.

Holley-Bockelmann et al. (2001) proposed a technique called ‘adiabatic squeezing’ to produce cuspy triaxial  $N$ -body models. They started with a spherical isotropic Hernquist model (Hernquist 1990) and eventually were applying a drag to the particle velocities along each principal axis. During the squeezing, the system retained its initial cuspy density profile with  $\gamma = 1$  and displayed a slight radial anisotropy in the velocity ellipsoid. Rodionov et al. (2008) described a very general prescription to construct a triaxial model by means of an iterative method (in original version proposed by Rodionov & Sotnikova 2006) and gave an example of such a model with a given density distribution and several constraints on kinematics.

All these techniques give us equilibrium or near equilibrium triaxial models but tell nothing about the nature of triaxiality. Triaxiality can arise in a number of ways. One natural way seen in hierarchical cosmological simulations is the merger of a number of objects. Moore et al. (2004) explored the generation of triaxial structures formed via merging isotropic equilibrium spherical haloes of NFW type with varying amounts of angular momentum. They investigated the relationship between the value of angular momentum and the final shape of configurations (prolate or oblate). Despite of the final shape their resulting haloes had the same density profile as the progenitor haloes, independent of their angular momentum.

Another common way of triaxial system formation is instability. Starting from equilibrium but unstable conditions a stellar system can achieve a new equilibrium that can be stable. The leading instability pushing the system towards a new equilibrium and rearranging its initial spherical density distribution into a triaxial one is the radial-orbit instability (Polyachenko & Shukhman 1981; for a physical description of this instability see Fridman & Polyachenko 1984). It manifests itself in systems with a high degree of velocity anisotropy (Merritt & Aguilar 1985; Meza & Zamorano 1997; Buyle et al. 2007). This instability is thought to be the main driver for the formation of elliptical galaxies (van Albada 1982). Sufficiently cold initial conditions force system stars to fall almost radially toward the centre. And if the system has too many radial orbits such a collapse will result in a triaxial configuration. Motivated by these ideas Trenti & Bertin (2006) fulfilled some numerical experiments to clarify the following questions: what kind of equilibria can be achieved in the process of the collisionless collapse starting from various conditions, what are the structural properties of the end-products and are they similar to the real galaxies.

In this paper we address to initially equilibrium spherical models with cusps and different degrees of the velocity anisotropy and analyse shapes, structure and kinematics of final triaxial configurations produced via radial-orbit instability.

The outline of this paper is as follows. In Section 2, we describe the technique for constructing initial equilibrium but non-stable cuspy  $N$ -body models with various degrees of velocity anisotropy and the  $N$ -body code used to study their evolution. In Section 3, we investigate the dynamical evolution of our models towards a new equilibrium and analyse their structure and kinematics. In Section 4, we discuss the properties of the final models in context of application to real stellar systems. In Section 5, we summarize our main results.

## 2. Modelling technique

### 2.1. Family of initial models

We start with cuspy spherical systems from the one-parameter family  $\gamma$ -models (Dehnen 1993; Tremaine et al. 1994). These models follow a density profile given by

$$\rho(r) = \frac{(3 - \gamma)a}{4\pi} \frac{M}{r^\gamma(r + a)^{4-\gamma}}, \quad (1)$$

where  $M$  — the total model mass and  $a$  — the typical scale length. The density of the models behaves as  $\rho \propto r^{-4}$  for large radii and as  $\rho \propto r^{-\gamma}$  near the centre, thus  $\gamma$  characterizes how a central cusp is strong.

We have limited our study to models with  $\gamma = 1$  (‘weak-cusp’) and  $\gamma = 3/2$  (‘moderate-cusp’). The former model is the so-called Hernquist sphere (Hernquist 1990). Surface density of both models is shown (Dehnen 1993) to agree quite well with the de Vaucoulers profile (de Vaucouleurs 1948) that describes the surface brightness of many ellipticals and bulges of spirals.

We considered a set of anisotropic models of the Osipkov-Merritt type (Osipkov 1979; Merritt 1985a,b). In this case the anisotropy parameter  $\beta = 1 - \sigma_t^2/2\sigma_r^2$ , where  $\sigma_t^2$  and  $\sigma_r^2$  are the tangential and radial components of the velocity dispersion, is a function of radius in the form (Osipkov 1979; Merritt 1985a,b)

$$\beta_{\text{OM}} = \frac{r^2}{r^2 + r_a^2}. \quad (2)$$

The anisotropy radius  $r_a$  cut off the isotropic core from the radial-orbit dominated region outside  $r_a$ .

Models with a given density distribution have two critical values for  $r_a$ . One value separates physical models with a strictly positive DF from unphysical ones. Another value marks the stability boundary. Merritt & Aguilar (1985); Meza & Zamorano (1997); Buyle et al. (2007) set numerically the stability threshold for various models including  $\gamma$ -models of Osipkov-Merritt type. For  $\gamma = 1$  the critical value of  $r_a$  is  $\approx 1.1$ , for  $\gamma = 3/2$  the stability threshold was found to be at  $r_a \approx 0.8$  (Meza & Zamorano 1997). We consider long time dynamical evolution of physical models lying below the stability threshold.

In all numerical simulations we used the following dimensionless units:  $G = 1$ ,  $M = 1$ ,  $a = 1$ . These units can be converted in physical ones through typical observational parameters of elliptical galaxies — mass and effective radius that characterizes the de Vaucoulers profile. For  $\gamma = 1$  effective radius  $r_e = 1.815a$  (Hernquist 1990), for  $\gamma = 3/2$  it can be derived from the cumulative surface density (Dehnen 1993)  $r_e = 1.276a$ . If we adopt  $M = 2 \cdot 10^{11} M_\odot$ ,  $r_e = 3$  kpc as typical parameters for bright ellipticals it will give us the scale unit  $r_u = a = 1.65$  kpc, the time unit  $t_u = 2.24$  Myr, the velocity unit  $v_u = 721.3$  km/s for  $\gamma = 1$ , and  $r_u = a = 2.35$  kpc,  $t_u = 3.80$  Myr,  $v_u = 604.7$  km/s for  $\gamma = 3/2$ .

Meza & Zamorano (1997); Buyle et al. (2007) expressed the evolution of their models in dimensionless units of half-mass dynamical time  $T_h$ . It is evaluated at the half-mass radius  $r_{1/2}$  (Binney & Tremaine 1987). For  $\gamma = 1$  it is equal  $T_h \approx 8.3$  and  $T_h \approx 4.9$  for  $\gamma = 3/2$ . Dehnen (1993) noticed that the ratio  $r_e/r_{1/2} \approx 0.75$  is practically the same for all  $\gamma$ -models. This means that if we fix the physical parameters (mass and effective radius) we will obtain the same physical dynamical time scale for all models. For  $\gamma = 1$  with adopted parameters it will be  $T_h = 18.7$  Myr and  $T_h = 18.8$  Myr for  $\gamma = 3/2$ .

We followed the dynamical evolution of the models further than in Meza & Zamorano (1997); Buyle et al. (2007), for some

models – up to  $t \approx 1000 - 1400$  (i.e.  $\approx (100 - 200)T_h$ ). It concerns the models just below the stability threshold. They were approaching the new steady state very slowly exhibiting a downfall to a new constant level in the behaviour of the axis ratio only after 70 – 120 dynamical times.

## 2.2. Initial data sets

An  $N$ -body realization of an initially spherically symmetric system was created in a conventional way by using the DF. For Osipkov-Merritt models the DF has a form

$$f(\mathcal{E}, L) = f(Q), \quad (3)$$

where  $Q = \mathcal{E} - L^2/2r_a^2$ ,  $\mathcal{E} = \Psi - \frac{1}{2}v^2$ ,  $\Psi$  is the negative of the gravitational potential, and  $L = rv_t$  is the angular momentum with  $v_t$  the tangential velocity components. The DF in the form (3) for a given density profile can be found through the technique (Osipkov 1979; Merritt 1985a,b) which is an extension of Eddington's (1916) inversion technique to obtain the DF for an isotropic spherical system.

The initial conditions in the  $N$ -body problem suggest specifying the mass, position in space, and three velocity components ( $v_r, v_\varphi, v_\theta$ ) for each particle.

The mass of all particles was assumed to be the same. As the DF is specified the particle positions and velocities are initialized by sampling the DF. The particle coordinates are naturally determined in accordance with the density profile (1). The usual way to do this is to invert the cumulative mass profile for the radius.

For velocity components it is enough to sample  $v_r$  and  $v_t = \sqrt{v_\varphi^2 + v_\theta^2}$  and to choose the random direction for  $v_t$  in the plane which is perpendicular to the radius-vector. The algorithm for velocity sampling in anisotropic systems of more general type than the Osipkov-Merritt models is briefly described in McMillan & Dehnen (2007) and implemented in the public code `mkhalo` which we have taken from the Walter Dehnen's part of the public NEMO package (<http://astro.udm.edu/nemo>; Teuben 1995).

## 2.3. Computational method

We investigated the dynamical evolution of our models by using the  $N$ -body code `gyrfalCON` (Dehnen 2000, 2002) that combines a hierarchical tree method (Barnes & Hut 1986) and a fast multipole method (Greengard & Rokhlin 1987). This code has complexity  $\mathcal{O}(N)$  and is faster than a standard tree code by at least a factor 10. Its implementation was taken from the public NEMO package (Teuben 1995).

For almost all models we chose the number of particles  $N = 300\,000$ . The tolerance parameter  $\theta$  that is responsible for the accuracy of calculating the gravitational force was fixed at 0.6 in all our simulations. Calculations were performed in a single-time-step mode. In this case momentum is exactly conserved. The time step and softening length were taken  $dt = 1/2^6$  and  $\epsilon = 0.04$ . The choice of these parameters was in agreement with the recommendations of Rodionov & Sotnikova (2005).

## 3. Properties of final equilibrium models

We performed the simulations on a long time scale (up to about 200 dynamical time for some models), and used the

temporal behaviour of the axis ratios  $b/a$  and  $c/a$  as indicators of new steady state settling. Till now such investigations were concentrated on finding numerically the stability threshold of spherical anisotropic models (Merritt & Aguilar 1985; Dejonghe & Merritt 1988; Meza & Zamorano 1997; Meza 2002; Buyle et al. 2007). Triaxial end-products formed due to the radial-orbit instability from initially equilibrium systems were commonly considered as a 'garbage'. Below we studied the structure and kinematics of such systems settled in a new equilibrium in details and determined the relationship between properties of initial and final models.

### 3.1. Model shapes

To determine the shape of the particle distributions we used a technique described by Dubinski & Carlberg (1991) and Katz (1991) (see also Meza & Zamorano 1997; Buyle et al. 2007). First of all we transformed the input  $N$ -body snapshot at specified time moments to a coordinate system which diagonalizes the moment of inertia tensor  $I_{ij} = \sum x_i x_j / r^2$  of a specified subset of particles within a certain sphere. For the sphere radius we chose  $r = 5$ . The centroid of the subset was translated to the origin. After diagonalization the principal components of the inertia tensor  $I_{xx} \geq I_{yy} \geq I_{zz}$  were used to calculate the preliminary values of the axis ratios

$$\frac{b}{a} = \left( \frac{I_{yy}}{I_{xx}} \right)^{1/2} \quad \text{and} \quad \frac{c}{a} = \left( \frac{I_{zz}}{I_{xx}} \right)^{1/2}. \quad (4)$$

After that we determined the ellipsoidal radius  $q$  as  $q = (x^2 + y^2/(b/a)^2 + z^2/(c/a)^2)^{1/2}$  and calculated the eigenvalues and eigenvectors of inertia tensor for a subset of particles with  $q \leq 5$ . Tensor components were found as  $I_{ij} = \sum (x_i x_j / q^2)$ . The new axis ratios were used as the conditions for the next iteration. We repeated this procedure until the error of both axial ratio determination became less than  $10^{-4}$ .

Figures 1 and 2 demonstrate the temporal behavior of the ratios between the intermediate and major axes and minor and major axes for two  $\gamma$ -models with different values of the anisotropy radius  $r_a$ .

Reaching the constant value of the axes ratio was considered as a new equilibrium. Some models with the anisotropy radius just below the stability threshold were approaching this state on a time scale longer than  $T_h = 50$ . As a result we obtained more extended end-products. For example, for  $\gamma = 1$  the stability threshold was set as  $r_a = 1.1$  (Meza & Zamorano 1997; Buyle et al. 2007). Starting from  $r_a = 1.05$  we have got after 150 dynamical times ( $t \approx 1200$ ) a perfectly prolate model with  $b/a, c/a \approx 0.77$ . The model with the anisotropy radius far from the stability threshold ( $r_a$ ) seems to be in nonequilibrium even after 100 dynamical times. A slow axes evolution is not noticeable on a short time scale ( $T_h = 50$ ) but is clearly seen during a longer period.

In the Table 1 we summarize the properties of all sets of simulations. The values of  $b/a$  and  $c/a$  are averaged over last 100 units of the time. They are very close to each other. It means that all the end-products of the initially unstable  $\gamma$ -models have an extremely prolate shape with a slight triaxiality for the model with  $\gamma = 1$  and  $r_a = 0.5$  and for the nonequilibrium model with  $\gamma = 1$  and  $r_a = 0.3$ .

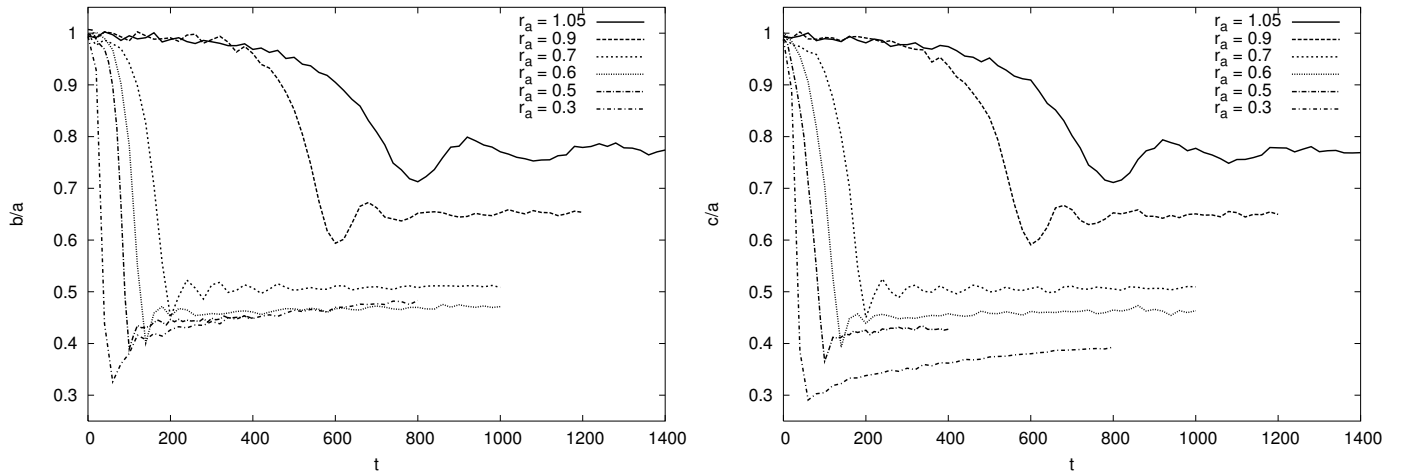


**Fig. 1.** Longtime evolution of the intermediate  $b$  and minor  $c$  to major  $a$  axis ratios for the  $\gamma = 1$  models with different values of initial anisotropy radius  $r_a$ . The axes lengths are iteratively calculated from the ellipsoidal density distribution using the moment of inertia tensor.

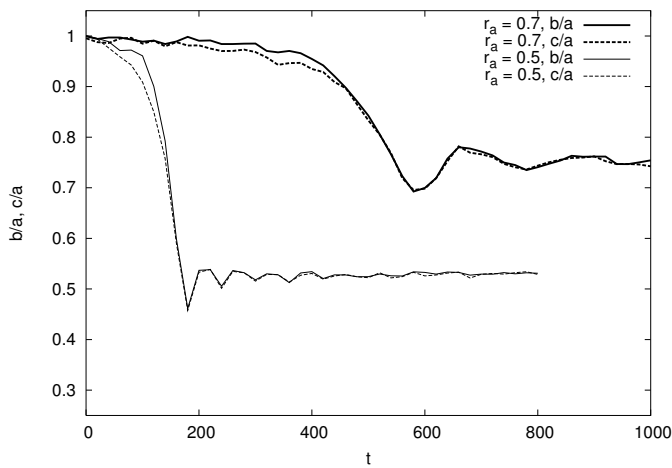


**Fig. 2.** Longtime evolution of the  $b/a$  and  $c/a$  ratios for the  $\gamma = 3/2$  models with two values of initial anisotropy radius  $r_a$ . The axes length are iteratively calculated from the ellipsoidal density distribution using the moment of inertia tensor.

**Table 1.** Properties of the final models

$\gamma$	$r_a$	$T_{\text{end}}$	$r_{a,f}$	$\delta$	$a$	$b/c$	$c/a$	$r_{a,f}/a$
1	1.05	1400	1.46	2.11	1.11	0.78	0.77	1.31
1	0.9	1200	1.59	2.07	1.24	0.65	0.65	1.29
1	0.7	1000	1.90	1.94	1.53	0.51	0.51	1.24
1	0.6	1000	2.00	1.79	1.83	0.47	0.46	1.10
1	0.5	400	2.08	1.79	1.93	0.45	0.43	1.07
1	0.3	800	1.91	1.64	2.03	0.48	0.39	0.94
3/2	0.7	1000	1.21	2.02	1.06	0.75	0.75	0.92
3/2	0.5	1000	0.97	2.09	1.44	0.53	0.53	0.84

### 3.2. Density profiles

The most remarkable feature of the end-products is their density profiles. During reaching a new equilibrium the  $\gamma$ -models retain their initial density profiles. Once the new scale length  $a$  is found

all density profiles of the final models can be described by a law like (1) but modified in the case of triaxiality as

$$\rho(q) = \frac{(3-\gamma)a^3}{4\pi bc} \frac{1}{q^\gamma(q+a)^{4-\gamma}}, \quad (5)$$

where  $q$  is ellipsoidal radius.

Figure 3 shows the density of the end-products as a function of an ellipsoidal radius  $q$ . We demonstrate also the fitting of some final density profiles by formula (5) with  $b/a$  and  $c/a$  taken at the end of simulations. The profiles can be fitted with an accuracy of better than 1%. The models exhibit an unchanging density profiles over  $\sim 3-4$  orders of magnitude in radius after settling to the new equilibrium, and they do not evolve away from the original cusps. The density slope seems to be an invariant feature of these models despite of their drastical rearranging into the triaxial configurations. Starting from a spherical model with a certain  $\gamma$  cusp we obtain a triaxial model with the cusp of the same shape.

### 3.3. Kinematics and velocity anisotropy

The velocity dispersions ( $\sigma_r$ ,  $\sigma_\varphi$ ,  $\sigma_\theta$ ) as a function of radius in Osipkov-Merritt models can be easily computed as the corresponding moments of the DF in the form  $f(Q)$  (Merritt 1985a,b). The  $\gamma$ -models of the Osipkov-Merritt type have a distinctive hump in their velocity dispersion profiles provided  $\gamma < 2$ . The same feature manifests itself in the radial profiles of the projected velocity dispersion (Carollo et al. 1995). The end-products exhibit the same hump in their velocity dispersion profiles like their spherical progenitors (Fig. 4). Despite of their nonspherical shape all models demonstrate the equivalency between  $v_\varphi$  and  $v_\theta$  velocity components as the spherical models with DF in the form  $f(\mathcal{E}, L)$ .

All final models display a radial anisotropy in the velocity ellipsoid. We choose to represent the anisotropy profiles with more general law than (2)

$$\beta = \frac{q^\delta}{q^\delta + r_{a,f}^\delta}, \quad (6)$$

with  $r_{a,f}$  and  $\delta$  being free parameters. The results of fitting are summarized in the Table 1. All models obtained from progeni-

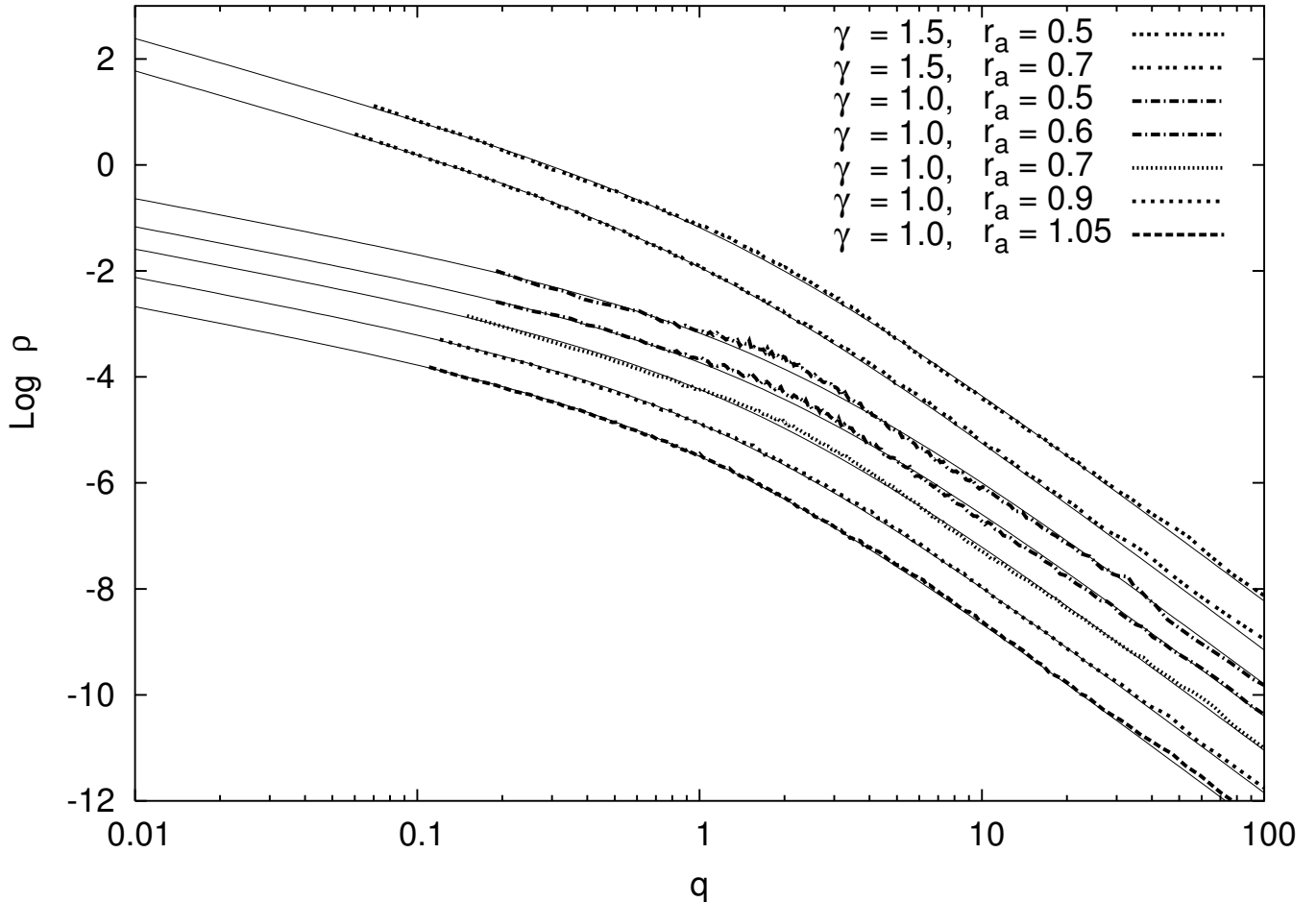


**Fig. 3.** Density of the models plotted as a function of ellipsoidal radius  $q$ . The curves show the density profiles for the final triaxial models formed via the radial-orbit instability from the initial  $\gamma$ -models with different values of anisotropy radius  $r_a$ . The thin solid lines show the fitting of profiles by formula (5). Curves are shifted from one another by dex=0.5 (from top to bottom) for convenience.

tors laying just below the stability threshold have the anisotropy profile with  $\delta \approx 2$ , e.g. they are of Osipkov-Merritt type. Fig 5 shows some examples. The profiles were fitted over the range  $q < 5$ . The deviation from (6) are observed only at large distances  $q > 5$  from the center and are due to a slight predominance of tangential orbits there as compared with Osipkov-Merritt models.

#### 4. Discussion

(1) Triaxial models formed due to instabilities from spherical anisotropic equilibrium systems were commonly thought as a ‘garbage’. Their structure and kinematics weren’t investigated in details. We showed that such models can be considered as equilibrium ones and used for studying their dynamical evolution and related topics concerned with dynamics of multicomponent systems.

(2) All our models have a near prolate shape without any strong triaxiality. Such a shape is a common feature of cosmologically motivated dark halos. There have been many theoretical papers published over the years which examined the subject of halo shapes. Most authors found that halos tend to be prolate. For example, using six high resolution dissipationless simulations with a varying box size in a flat LCDM universe Allgood et al. (2007) found that most halos in their simulations

were prolate in shape with very few oblate halos. But our prolate models, that are based on initial spherically symmetric  $\gamma$ -models, are rather suit to describing the density distribution of ellipticals and bulges.

Several authors discussed the problem of the intrinsic shape of elliptical galaxies (e.g., Franx et al. 1991; Vincent & Ryden 2005; Padilla & Strauss 2008). Many of them agree that the observed distribution of ellipticities can be reproduced by suggesting the triaxiality of these objects. It is concluded that any acceptable distribution is dominated by nearly-oblate spheroidal rather than nearly-prolate spheroidal systems. Padilla & Strauss (2008) have recently reexamined the underlying shapes of elliptical galaxies in the SDSS Data Release 6 from the observed distribution of projected galaxy shapes, taking into account the effects of dust extinction and reddening. The elliptical galaxy data were found to be consistent with oblate spheroids, with a correlation between luminosity and ellipticity: more luminous ellipticals tend to be rounder, although ellipticals are oblate at all luminosities. This result is in agreement with an analysis by Vincent & Ryden (2005) based on SDSS Data Release 3 although later authors found that the fainter de Vaucouleurs galaxies are best fitted with prolate spheroids with mean axis ratio  $\langle(b, c)/a\rangle \approx 0.51$ .

Méndez-Abreu et al. (2008) performed two-dimensional photometric decomposition of the galaxy surface brightness dis-

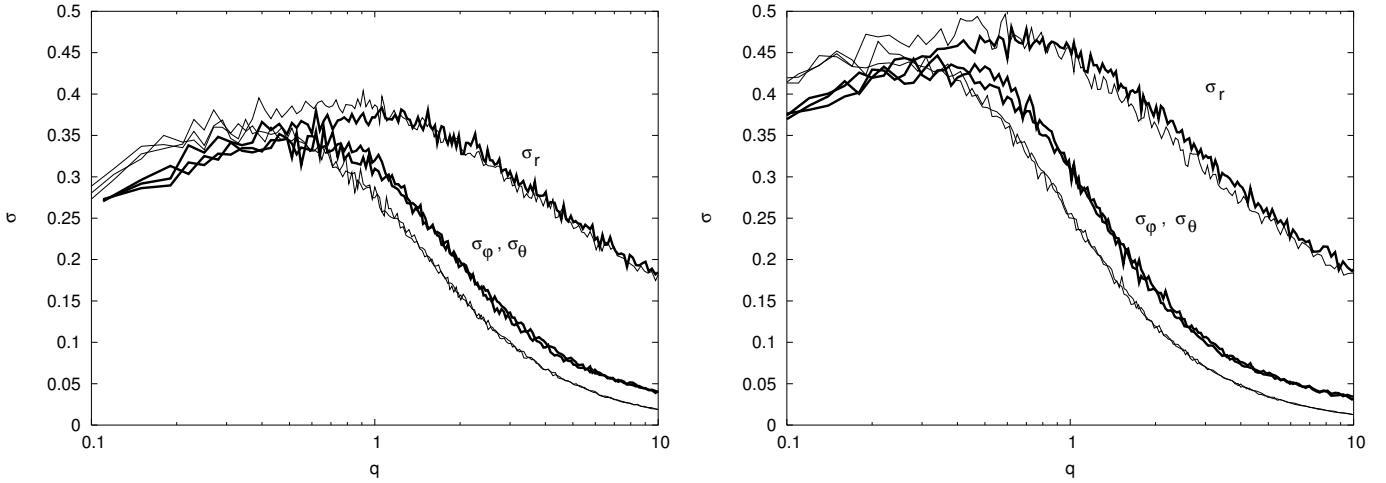


**Fig. 4.** The dependance of three moments of the velocity distribution, namely  $\sigma_r$ ,  $\sigma_\varphi$  and  $\sigma_\theta$ , as a function of ellipsoidal radius  $q$ . Thin curves — the initial profiles, thick curves — the profiles for end-products. Left —  $\gamma = 1$ ,  $r_a = 1.05$ ; right —  $\gamma = 3/2$ ,  $r_a = 0.7$ .

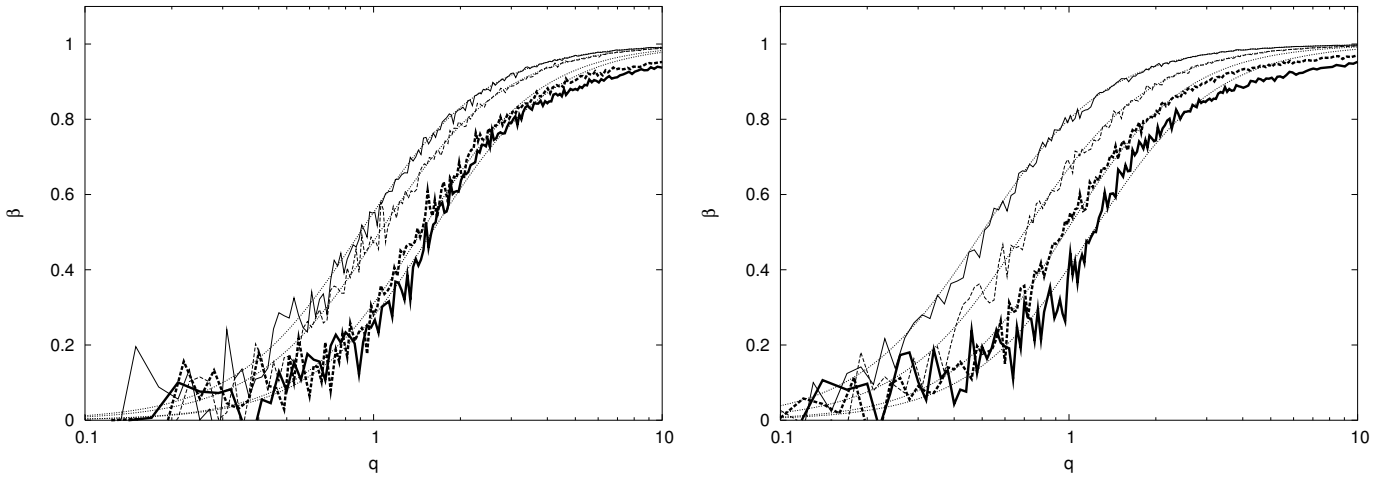


**Fig. 5.** The velocity anisotropy parameter as a function of ellipsoidal radius  $q$ . Thin curves — the initial profiles, thick curves — the profiles for end-products, thin dotted lines show profiles obtained by fitting the data by formula (6). Left —  $\gamma = 1$ ; solid lines —  $r_a = 0.9$ , dashed lines  $r_a = 1.05$ . Right —  $\gamma = 3/2$ , solid lines —  $r_a = 0.5$ , dashed lines  $r_a = 0.7$ .

tribution to derive the structural parameters of disks and bulges for 148 unbarred S0-Sb galaxies. They obtained the probability distribution function of the intrinsic equatorial ellipticity of bulges and found that about 80% of bulges in their sample are not oblate but triaxial spheroids. This is consistent with several previous findings.

Thus, in the context of observational data our models can be related only with the lowest luminosity ellipticals.

(3) All our final models are strongly elongated with  $\langle (b, c)/a \rangle \approx 0.5 - 0.8$ . It's true even for the models starting from the conditions just below the level of stability. For  $r_a = 1.05$  we followed the dynamical evolution of the system further ( $T_{\text{end}} \approx 170T_h$ ) than it was done by Meza & Zamorano (1997) and Buyle et al. (2007) and obtained a very elongated end-product.

(4) One of the main points of our investigation is that the shape of the density profile didn't change. The end-product structure can be predicted in a quite definite way and depends only on initial model properties. Moore et al. (2004) noticed that their triaxial remnants formed via merging keep central density slopes of progenitors. Boylan-Kolchin & Ma (2004) claimed

that if the cuspy halo had started out with an NFW form with  $\gamma = 1$ , the merged halo also had a form close to NFW one, with a slightly shallow inner cusp of  $\rho \propto r^{-0.7}$  instead of  $r^{-1}$ . Holley-Bockelmann et al. (2001), who had used a squeezing technique for constructing triaxial systems, also concluded that their models retained the given  $\gamma$  character after squeezing had terminated. It seems the cusp shape is an invariant feature of any matter rearranging as though the particles retain the memory of the progenitor density profile.

(5) The dark halos obtained in cosmological simulations have a small degree of anisotropy far from the center (Cole & Lacey 1996; Colín et al. 2000; Fukushige & Makino 2001; Diemand et al. 2004). We know a little about 3D velocity distributions in ellipticals. But modern methods for modelling of observational data allow to reconstruct such distributions. Combining surface brightness photometry and long-slit absorption line kinematic data, De Lorenzi et al. (2008) have recently presented a dynamical study of NGC 4697, intermediate-luminosity, E4 galaxy. Their best fitting models were only slightly radially anisotropic, with the anisotropy parameter increasing to  $\beta \approx 0.5$  at large radii.

The kinematic properties of the prolate models under study aren't similar to the properties of the cosmological dark halos and ellipticals. The possible explanation is that we started out from very anisotropic models of the OM type. The velocity anisotropy profile on the periphery was produced by purely radial orbits ( $\beta$  tends to 1). The end-products are also anisotropic at large radii but  $\beta$  is less than 1 (see Fig 5). However, as one can see from the Table 1, the size of the isotropic core increased for all models and once rescaled it corresponds to the value for marginally stable  $\gamma$ -progenitors and almost independent on a starting unstable point. As opposed to this picture, in a merging scenario the particle velocities, being initially isotropic, remain mostly isotropic near the centre of the merger remnant, but become mildly anisotropic ( $\beta < 0.4$ ) with increasing radius due to radial infalls (Boylan-Kolchin & Ma 2004).

Velocity dispersion profiles of our models demonstrate one remarkable feature — the equivalency between  $v_\varphi$  and  $v_\theta$  velocity components. This fact in combination with a model shape may help to construct the DF of such prolate systems in the form  $f(\mathcal{E}, L)$ .

(6) We followed the evolution of our models further than in previous investigations (Meza & Zamorano 1997; Buyle et al. 2007). These authors studied the stability of their models by using an  $N$ -body code based on the 'self-consistent field' method (Hernquist & Ostriker 1992), in which the density and the gravitational potential are expanded in a biorthogonal set of some basis functions. The using of spherical harmonics provided a reflection symmetry. We used a tree-like code (Teuben 1995; Dehnen 2000, 2002) and reached a definitive equilibrium only by a special symmetrization procedure that preserves a reflection symmetry of a model during a simulation (the manipulator `symmetrize` in Dehnen's `gyrfalcoN`). One have to keep this fact in mind when modelling such systems.

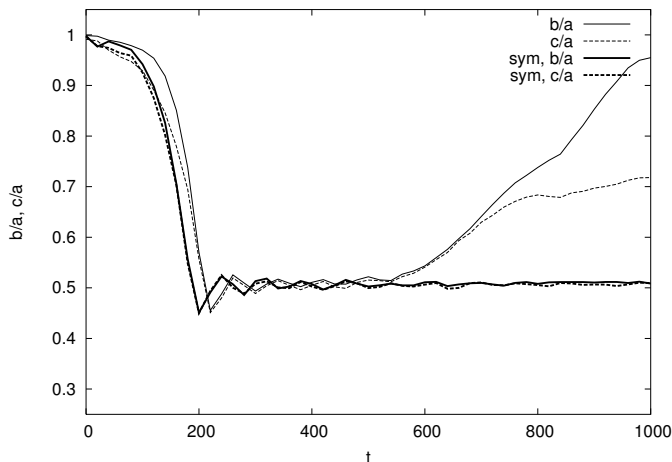


**Fig. 6.** Longtime evolution of the  $c/a$  ratio for the  $\gamma = 1$  models with  $r_a = 0.7$ . Thin curves — calculations without symmetrization, thick curves — calculations with `symmetrize` manipulator. The axes length are iteratively calculated from the ellipsoidal density distribution using the moment of inertia tensor.

(7) Merritt & Fridman (1996); Merritt (1997) considered the question about the degree to which triaxiality can be supported in galaxies with high central densities. They concluded that triaxiality is inconsistent with a strong cusp due to rapid chaotic mixing and a real galaxy might choose axisymmetry with a tendency to be nearly prolate spheroidal, nearly prolate, or nearly

spherical. All our models formed via the radial orbit instability are axisymmetric with a prolate shape. This form is reached on a time scale of about  $\sim 50 T_h$ . After that it can be preserved only by a 'hand-made' maintenance of a reflection symmetry. Without this maintenance some of our systems undergo the instability and start evolving towards nearly oblate spheroids (see Figure 6). It is known that instability criteria are the strongest constraints on structural and kinematic parameters of stellar systems and instability is a natural way for equilibrium stellar system formation. That is why the models constructed here need further investigations. Further studies will analyse the long time orbital evolution of particles to study orbit families consisting these models and the degree of chaos.

## 5. Summary

Our results can be summarized as follows:

1. The radial orbit instability is a natural way to build nonspherical systems and can be considered as a new technique for constructing equilibrium  $N$ -body models.
2. These models have quite predictable properties because the shape of the density profiles doesn't change in the process of instability. For example, the initial cusp survives.
3. New steady state models have a definitely prolate shape.
4. The degree of anisotropy is diminishing and end-products are more isotropic.

*Acknowledgements.* This work was partially supported by the Russian Foundation for Basic Research (grant 06-02-16459) and by grant from President of the Russian Federation for support of Leading Scientific Schools (grant NSH-8542.2006.02).

## References

- Aguilar L.A., Merritt D., 1990, *ApJ*, 354, 33  
 Allgood B., Flores R.A., Primack J.R., Kravtsov A.V., Wechsler R.H., Faltenbacher A., Bullock J.S., 2007, *MNRAS*, 367, 1781  
 Baes M., Dejonghe H., 2002, *A&A*, 393, 485  
 Baes M., Van Hese E., 2007, *A&A*, 471, 419  
 Bailin J., Steinmetz M., 2005, *ApJ*, 627, 647  
 Barnes J., Hut P., 1986, *Nature*, 324, 446  
 Bett Ph., Eke V., Frenk C., Jenkins A., Helly J., Navarro J., 2007, *MNRAS*, 376, 215  
 Binney J., Tremaine S., 1986, *Galactic Dynamics*. Princeton Univ. Press, Princeton  
 Boily C.M., Kroupa P., & Peñarrubia-Garrido J., 2001, *New A*, 6, 27  
 Boylan-Kolchin M., Ma C.-P., 2004, *MNRAS*, 349, 1117  
 Buyle P., Van Hese E., De Rijcke S., Dejonghe H., 2007, *MNRAS*, 375, 1157  
 Capuzzo-Dolcetta R., Leccesse L., Merritt D., Vicari A., 2007, *ApJ*, 666, 165  
 Carollo C.M., de Zeeuw P.T., van der Marel R.P., 1995, *MNRAS*, 276, 1131  
 Cole Sh., Lacey C., 1996, *MNRAS*, 281, 716  
 Colín P., Klypin A.A., Kravtsov A.V., 2000, *ApJ*, 539, 561  
 Cuddeford P., 1991, *MNRAS*, 253, 414  
 Dehnen W., 2000, *MNRAS*, 265, 250  
 Dehnen W., 2000, *ApJ*, 536, 39  
 Dehnen W., 2002, *Journal of Computational Physics*, 179, 27  
 De Lorenzi F., Gerhard O., Saglia R.P., Sambhus N., Debattista V.P., Panella M., Méndez R.H., 2008, *MNRAS*, 385, 1729  
 Diemand J., Moore B., Stadel J., 2004, *MNRAS*, 352, 535  
 Dejonghe H., Merritt D., 1988, *ApJ*, 328, 93  
 de Vaucouleurs G., 1948, *Ann. Astrophys.*, 327, L55  
 Dubinski J., Carlberg R.G., 1991, *ApJ*, 378, 496  
 Eddington A.S., 1916, *MNRAS*, 76, 572  
 Ferrarase L., van den Bosch F.C., Ford H.C., Jaffe W., O'Connell R.W., 1994, *AJ*, 108, 1598  
 Frenk C.S., White S.D.M., Davis M., Efstathiou G., 1988, *AJ*, 327, 507  
 Franx M., Illingworth G., de Zeew T., 1991, *ApJ*, 383, 112  
 Fridman A.M., Polyachenko V.L., 1984, *Physics of Gravitating Systems*. Springer-Verlag, New York  
 Fukushige T., Makino J., 2001, *ApJ*, 557, 533

- Greengard L., Rokhlin V., 1987, *Journal of Computational Physics*, 73, 325  
Hernquist L., 1990, *ApJ*, 356, 359  
Hernquist L., 1993 *A&AS*, 86, 389  
Hernquist L., Ostriker J.P., 1993 *ApJ*, 386, 375  
Holley-Bockelmann K., Mihos J.C., Sigurdsson S., Hernquist L., 2001, *ApJ*, 549, 862  
Jing Y.P., Suto Y., 2002, *ApJ*, 574, 538  
Katz N., 1991, *ApJ*, 368, 325  
Kuijken K., Dubinski D., 1995, *MNRAS*, 277, 1341  
Lauer T.R., 1995, *AJ*, 110, 2622  
McMillan P.J., Dehnen W., 2007, *MNRAS*, 378, 541  
Mendez-Abreu J., Aguerrri J.A.L., Corsini E.M., Simonneau E., 2008, *â*, 487, 555  
Merritt D., 1985, *AJ*, 90, 1027  
Merritt D., 1985, *MNRAS*, 214, 25  
Merritt D., 1997, *ApJ*, 486, 102  
Merritt D., Aguilar L.A., 1985, *ApJ*, 217, 787  
Merritt D., Fridman T., 1996, *ApJ*, 460, 136  
Meza A., 2002, *â*, 395, 25  
Meza A., Zamorano N., 1997, *ApJ*, 490, 136  
Moore B., Kazantzidis S., Diemand J., Stadel J., 2004, *MNRAS*, 354, 522  
Navarro J.F., Frenk C.S., White S.D.M., 1996, *ApJ*, 462, 563  
Navarro J.F., Frenk C.S., White S.D.M., 1997, *ApJ*, 490, 493  
Osipkov L.P., 1979, *Soviet Astronomy Letters*, 5, 42  
Padilla N.D., Strauss M.A., 2008, *MNRAS*, 388, 1321  
Polyachenko V.L., Shukhman I.G., 1981, *Soviet Astronomy*, 25, 533  
Rodionov S.A., Sotnikova N.Ya., 2005, *Astron. Rep.*, 49, 470  
Rodionov S.A., Sotnikova N.Ya., 2006, *Astron. Rep.*, 50, 983  
Rodionov S.A., Athanassoula L., Sotnikova N.Ya. 2008, *MNRAS*, submitted  
Schwarzschild M., 1979, *ApJ*, 232, 236  
Shaw L.D., Weller J., Ostriker J.P., Bode P., 2005, *ApJ*, 646, 815  
Statler T., 1987, *ApJ*, 321, 113  
Teuben P.J., 1995, in *ASP Conf. Ser. 77, Astronomical Data Analysis Software and Systems IV*, ed. Shaw R.A., Payne H.E., Hayes J.J.E., 398  
Tremaine S., Richstone D.O., Yong-Ik B., Dressler A., Faber S.M., Grillmair C., Kormendy J., Lauer T.R., 1994, *AJ*, 107, 634  
Trenti M., Bertin G., 2006, *ApJ*, 637, 717  
van Albada T.S., 1982, *MNRAS*, 201, 939  
Vincent A.R., Ryden B.S., 2005, *ApJ*, 623, 137  
Warren M.S., Quinn P.J., Salmon J.K., Zurek W.H., 1992, *ApJ*, 399, 405  
Widrow L.M., Dubinski D., 2005, *ApJ*, 631, 838